RESEARCH ARTICLE | JUNE 28 2024

Chemically reactive and aging macromolecular mixtures. I. Phase diagrams, spinodals, and gelation

Ruoyao Zhang ; Sheng Mao ; Mikko P. Haataja

J. Chem. Phys. 160, 244903 (2024)
https://doi.org/10.1063/5.0196793

The Journal of Chemical Physics ARTICLE pubs.aip.org/aip/jcp

Chemically reactive and aging macromolecular mixtures. I. Phase diagrams, spinodals, and gelation

Cite as: J. Chem. Phys. 160, 244903 (2024); doi: 10.1063/5.0196793
Submitted: 9 January 2024 • Accepted: 24 May 2024 •
Published Online: 28 June 2024

Ruoyao Zhang,[1] Sheng Mao,[2,a)] and Mikko P. Haataja[1,3,4,a)]

AFFILIATIONS

[1] Department of Mechanical and Aerospace Engineering, Princeton University, Princeton, New Jersey 08544, USA
[2] Department of Mechanics and Engineering Science, College of Engineering, Peking University, Beijing 100871, China
[3] Princeton Materials Institute, Princeton University, Princeton, New Jersey 08544, USA
[4] Omenn-Darling Bioengineering Institute, Princeton University, Princeton, New Jersey 08544, USA

[a)] **Authors to whom correspondence should be addressed:** maosheng@pku.edu.cn and mhaataja@princeton.edu

ABSTRACT

Multicomponent macromolecular mixtures often form higher-order structures, which may display non-ideal mixing and aging behaviors. In this work, we first propose a minimal model of a quaternary system that takes into account the formation of a complex via a chemical reaction involving two macromolecular species; the complex may then phase separate from the buffer and undergo a further transition into a gel-like state. We subsequently investigate how physical parameters such as molecular size, stoichiometric coefficients, equilibrium constants, and interaction parameters affect the phase behavior of the mixture and its propensity to undergo aging via gelation. In addition, we analyze the thermodynamic stability of the system and identify the spinodal regions and their overlap with gelation boundaries. The approach developed in this work can be readily generalized to study systems with an arbitrary number of components. More broadly, it provides a physically based starting point for the investigation of the kinetics of the coupled complex formation, phase separation, and gelation processes in spatially extended systems.

I. INTRODUCTION

Traditionally, the intracellular organization of organelles has been associated with compartments, which are surrounded by membranes. Modern imaging approaches indicate, however, that membraneless organelles exist outside of this classical view.[1] These organelles are typically micron-sized clusters comprised of macromolecules such as RNAs and proteins, which may emerge via liquid–liquid phase separation (LLPS), forming droplets ("biomolecular condensates").[2] More intriguingly, the dynamics of these initially liquid-like condensates often slow down over time, exhibiting viscoelastic or even solid-like properties.[3,4] This time-dependent liquid-to-solid-like transition ("aging") is a characteristic behavior associated with several neurodegenerative diseases such as Alzheimer's disease, Parkinson's disease, and amyotrophic lateral sclerosis (ALS), among others.[5] Therefore, in recent years, aging has begun to receive attention in the study of intracellular phase separation.

In general, the scope of LLPS can be expanded from binary solutions to a broad range of mixtures in which multiple macromolecular species interact with each other. The formation of complex coacervates and the subsequent LLPS by mixing multiple multivalent, oppositely charged molecules are rather well characterized by now.[6,7] Bracha *et al.* designed an oligomerizing biomimetic system ("Corelets") to investigate the effects of multivalent interactions of intrinsically disordered protein regions (IDPs/IDRs) on LLPS.[8] In their system, a spherical core with multiple photo-activatable domains recruits proteins when light shines upon it. The new complex structure formed by the core and proteins behaves distinctly from its constituents, and it can in turn aggregate and phase separate from the buffer solution to form a liquid condensate. One can perceive this activation/deactivation process as a reversible light-

induced chemical reaction. In fact, a number of experiments have already shown that macromolecules with different sizes and lengths, such as colloid–polymer solutions,[9] cholesterol and phospholipid systems,[10] protein–DNA,[11,12] and enzyme–protein mixtures,[13,14] can readily react to form condensates. Theoretical works by Corrales and Wheeler,[15] and Talanquer[16] were the first to consider a reversible chemical reaction between the binary components of a liquid mixture to produce a third liquid component, which was subsequently phase-separated from the reactant species. Radhakrishnan and McConnell[10,17,18] further extended this idea to the non-ideal mixing behavior of cholesterol and reactive and unreactive phospholipids, demonstrating that such models can be readily applied to systems of biological relevance. More recently, following the approach of Bazant,[19,20] Kirschbaum and Zwicker formulated a thermodynamically consistent model to study chemical reactions in the context of biomolecular condensates while accounting for different molecular volumes of the reactants.[21]

It is important to note that existing mesoscale theoretical models of multi-component LLPS, or reaction-induced phase separation,[21,22] assume all species to be in a liquid state, thus ignoring any aging processes, which often have great physical significance in both polymer solutions and biomolecular systems. Aging can be caused by different types of microstructural changes, such as physical gelation and fibril formation. For example, a gelatin–methanol–water mixture can lead to phase separation and gelation;[23] colloid–polymer solutions can undergo gelation;[9] and protein condensates show solid-like properties and various non-spherical morphologies during aging.[24,25] To partially address the role of aging on LLPS, Berry *et al.* proposed a minimal mesoscale kinetic model for coupled ternary phase separation, gelation, and chemical reactions[26] but did not provide quantitative results. Therefore, a theoretical framework to study the coupled processes of chemical reaction, phase separation, and aging may help facilitate the development of a better understanding of ALS-like diseases, as well as many other similar systems more generally.

As a step toward this goal, we mainly focus on the thermodynamic equilibrium properties of a multicomponent, reactive macromolecular system in this paper. To this end, we first propose a minimal model of a quaternary mixture by constructing a free energy that incorporates chemical reactions and phase separated liquid-like states. Based on the free energy model, we then compute the corresponding phase diagrams to study the phase behavior of the mixture and its propensity to undergo aging via gelation. We systematically investigate how physical parameters such as stoichiometric coefficients, molecular sizes, equilibrium constants, and interaction parameters affect the equilibrium properties of the mixture. A detailed study of the coupled diffusive kinetics, chemical reactions, and aging behavior will be presented in a separate publication.[27]

II. THERMODYNAMIC MODEL

Let us consider an initially ternary system composed of species X, Y, and B. Among the three species, B denotes the buffer in which X and Y are immersed. Species X and Y are chemically reactive and may form a complex X_nY_m (denoted by Z) via the following reversible reaction:

$$nX + mY \leftrightarrow X_nY_m \equiv Z, \tag{1}$$

where n and m denote stoichiometric coefficients. The four molecular species defined by their respective volume fractions, X, Y, Z, and B, form a liquid mixture at equilibrium. The mixture is taken to be incompressible such that $B = 1 - X - Y - Z$. The molecular volume of the ith species is taken to be $v_i = r_i v_{i,0}$, where r_i and $v_{i,0}$ denote the degree of polymerization and monomer volume, respectively, as different polymers may have different monomer volumes. The volume conservation of Eq. (1) then leads to $v_z = nv_x + mv_y$.[21] Figure 1 illustrates a reaction between two molecules and one long polymer

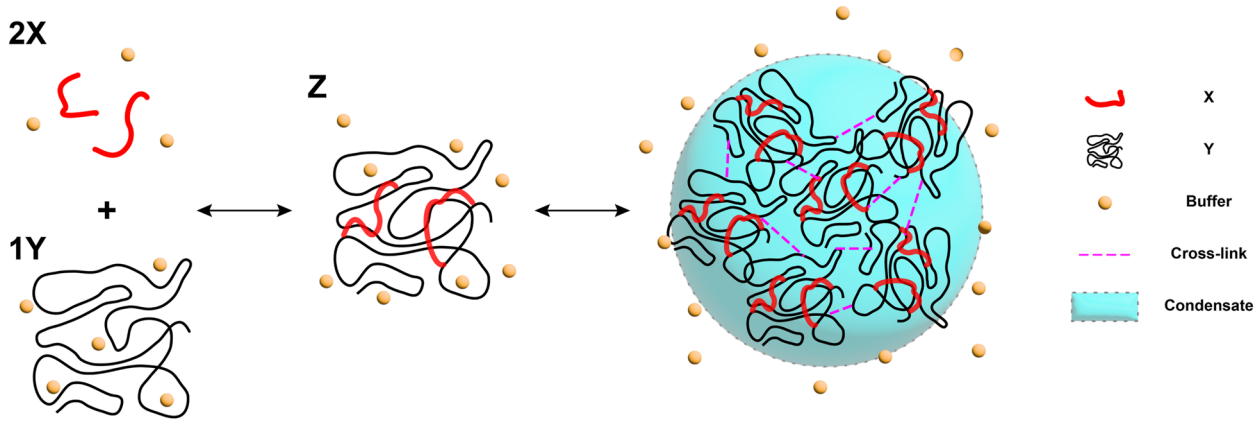

FIG. 1. Schematic of the reactive macromolecular mixture considered in this work. Two species, X and Y, react to form a complex, Z, which subsequently separates from the buffer. The complexes may subsequently undergo physical crosslinking, leading to gelation. The stoichiometric coefficients are set to $n = 2$ and $m = 1$ in this example.

chain to form a complex. The complexes subsequently aggregate to form a macroscopic condensate via LLPS.

Following the approach of Radhakrishnan and McConnell,[10] we consider a free energy density for the liquid mixture,

$$f_{\text{liquid}}(X,Y,Z) = \mu_x^0 + \frac{X}{r_x}\ln X + \mu_y^0 + \frac{Y}{r_y}\ln Y + \frac{Z}{r_z}\left(\ln Z + \mu_z^0\right) + B\ln B + \chi_{xy}XY + \chi_{xz}XZ + \chi_{yz}YZ + \chi_{xb}XB + \chi_{yb}YB + \chi_{zb}ZB. \quad (2)$$

In this model, all standard chemical potentials μ_i^0 are constant and set equal to zero for convenience, with the exception of the complex, $\mu_z^0 = -\ln K$, where the parameter K corresponds to the equilibrium constant for the reaction[10,17,18] in an ideal solution ($\chi_{ij} = 0$) with equal degrees of polymerization. The interaction parameters χ_{ij} determine whether two different species (i and j) attract or repel each other, which governs the global mixing/demixing behaviors. Finally, if one considers only the change in the translational entropy associated with the complexes, $r_z = nr_x + mr_y$; however, to allow for possible changes in chain conformations upon complex formation, r_x, r_y, and r_z are treated as independent parameters.

Phase separation of polymers in solution may, in addition, induce strong associations in the form of cross-links between segments of the polymer chains, leading to the formation of a thermoreversible, physical gel.[23,28] To incorporate gelation of macromolecular mixtures into our model, the liquid-to-gel transition within clusters of molecular complexes is captured using a simple criterion: gelation commences when $Z > Z^*$, where Z^* is proportional to the critical cross-linking volume fraction necessary to form a gel.[29]

III. EQUILIBRIUM BEHAVIOR

A. Phase diagrams

A phase diagram is a useful tool for understanding the equilibrium states of complex mixtures, including phase coexistences and the nature of phase transitions (e.g., continuous vs discontinuous). While multi-component phase diagrams have been widely used in the field of materials science, a rather limited number of works have used them to study biological and/or chemically reactive systems. For example, Horst and Wolf proposed a numerical method for constructing phase diagrams for quaternary polymer blends.[30] Veatch and Keller mapped the phase boundaries of the DPPC/DOPC/Chol mixture on a ternary phase diagram.[31] Radhakrishnan and McConnell calculated the phase diagram for cholesterol and two phospholipids, highlighting the two-phase coexistence region.[18] In more recent work, Shin and Brangwynne proposed a hypothetical phase diagram for protein condensates, which incorporates phase coexistence and phase transitions between liquid, disordered "glassy," and solid/crystalline states.[3]

To better understand the interplay between LLPS, chemical reactions, and aging, we proceed to construct phase diagrams of the effective quaternary mixture described in the previous section. We begin by looking at a ternary mixture of X, Y, and B, that is, a reactive system that has no complexes present initially. Following the treatment of Radhakrishnan and McConnell,[10] we first introduce a reaction progress parameter γ (proportional to the complex volume fraction) to calculate the final volume fraction of the complex Z, assuming that the reaction attains equilibrium. Now, for a given γ, f_{liquid} can be expressed as

$$f_{\text{liquid}}(X_0,Y_0,\gamma) = \frac{(X_0 - n\nu_x\gamma)}{r_x}\ln(X_0 - n\nu_x\gamma) + \frac{(Y_0 - m\nu_y\gamma)}{r_y}\ln(Y_0 - m\nu_y\gamma) + \frac{\nu_z\gamma}{r_z}[\ln(\nu_z\gamma) - \ln K] + (1 - X_0 - Y_0)\ln(1 - X_0 - Y_0) + \chi_{yz}\nu_z\gamma(Y_0 - m\nu_y\gamma) + \chi_{xy}(X_0 - n\nu_x\gamma)(Y_0 - m\nu_y\gamma) + \chi_{xz}\nu_z\gamma(X_0 - n\nu_x\gamma) + [\chi_{xb}(X_0 - n\nu_x\gamma) + \chi_{yb}(Y_0 - m\nu_y\gamma)](1 - X_0 - Y_0) + \chi_{zb}\nu_z\gamma(1 - X_0 - Y_0), \quad (3)$$

where X_0 and Y_0 denote the initial volume fractions of X and Y, respectively. We note that $0 \le \gamma \le \min\left(\frac{X_0}{n\nu_x}, \frac{Y_0}{m\nu_y}\right)$. The phase diagrams are constructed by first minimizing $f_{\text{liquid}}(X_0,Y_0,\gamma)$ with respect to γ for given X_0 and Y_0 to yield $\gamma_{\min} = Z/\nu_z$; the minimization is carried out numerically as the resulting expression, in general, does not yield a closed-form analytical solution for $\gamma_{\min}$. Then, from the free energy function $f_{\text{liquid}}(X_0,Y_0,\gamma_{\min})$, we compute the ternary phase diagram by convexifying it using an algorithm based on the convex-hull construction.[22,32] The algorithm not only determines the phase coexistence regions but also automatically generates tie-lines in those regions, thus determining the equilibrium compositions and complex volume fractions. On the resulting phase diagram, the gelation regions are shaded in gray for regions where $Z > Z^*$. Gelation will be induced if the final volume fraction of the complex of at least one of the coexisting phases exceeds Z^*. We note that a full treatment of the spatio-temporal dynamics of the coupled complex formation, phase separation, and gelation processes is required to fully characterize the behavior of the system in this regime.

Inspired by experiments on protein–DNA coacervates,[11,12] let us use the following simple system as an example, in which there only exists a repulsive interaction between Z and the buffer, controlled by a positive χ_{zb} parameter, while all other interaction parameters χ_{ij} are set to zero. That is, while X, Y, and the buffer form an ideal liquid mixture, the complex Z is primed to phase separate from the buffer and potentially form a gel. We set $n = m = 1$, $\nu_x = \nu_y = 1$, $r_x = r_y = 1$, $r_z = 2$, and $\chi_{zb} = 4$, $K = 100$, and $Z^* = 0.7$; the corresponding phase diagram is shown in Fig. 2(a).[33] The white areas represent two-phase coexistence regions, in which the mixture will phase separate into a complex-poor and complex-rich phase as dictated by the tie-lines (dashed lines). In Fig. 2(a), three representative initial compositions of X_0 and Y_0 are highlighted, i.e., (0.1, 0.25), (0.1, 0.45), and (0.1, 0.8) as red, blue, and green stars, respectively. Each of these systems yields a distinct equilibrium state. The mixture initiated at the red star will phase separate and undergo gelation in the condensed complex phase as the right end of the tie-line enters the gelation region; the mixture initiated at the blue star will phase separate without experiencing any gelation; and initializing the system at the green star yields a homogeneous liquid solution with no gelation.

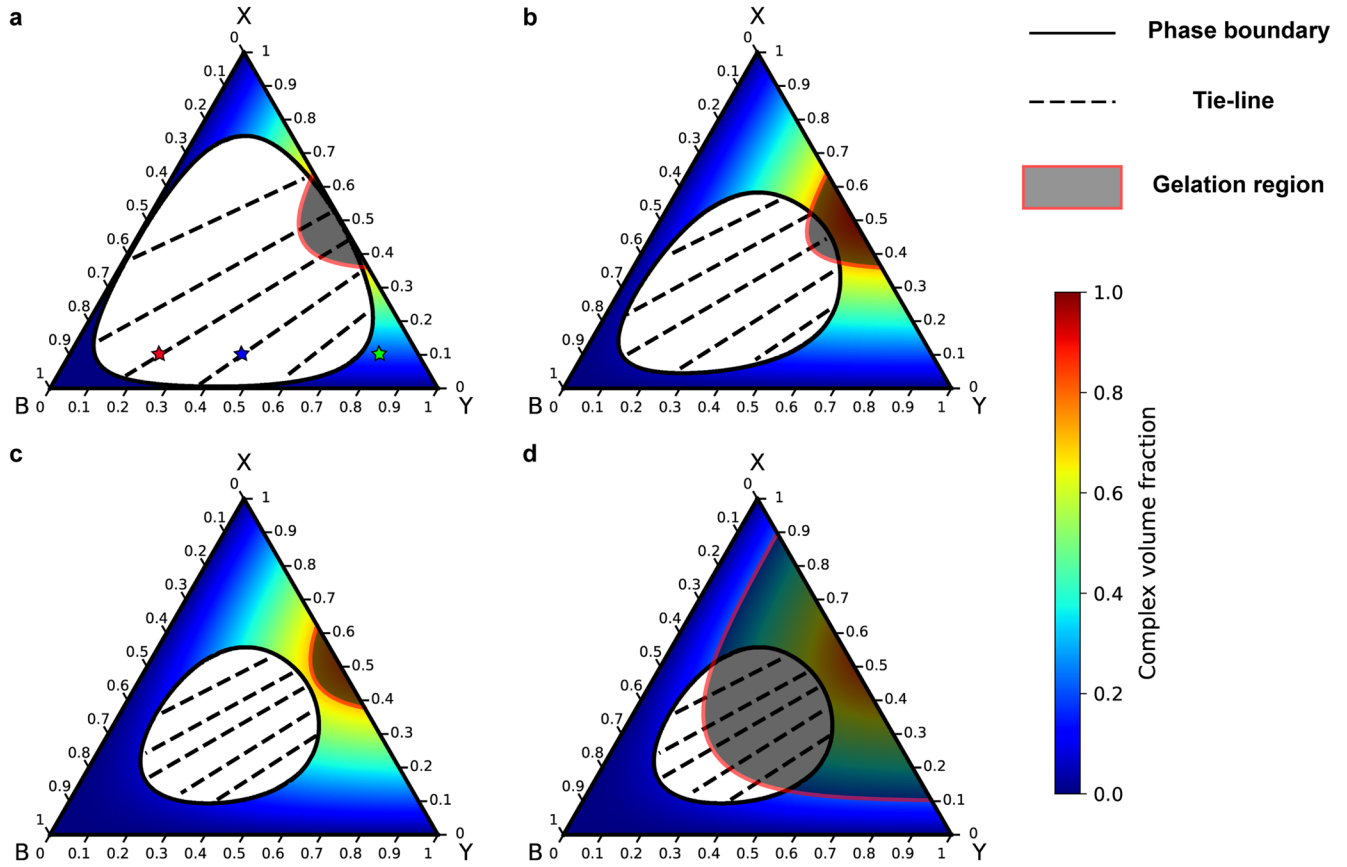

FIG. 2. Effects of varying interaction parameters, equilibrium constants, and gelation criteria on the phase behavior of the quaternary mixture at fixed stoichiometry ($n = m = 1$), molecular volumes ($v_x = v_y = 1$, $v_z = 2$), and degrees of polymerization ($r_x = r_y = 1, r_z = 2$). The interaction parameter, equilibrium constant, and gelation criterion were set to (a) $\chi_{zb} = 4$, $K = 100$, and $Z^* = 0.7$; (b) $\chi_{zb} = 2.5$, $K = 100$, and $Z^* = 0.7$; (c) $\chi_{zb} = 2.5$, $K = 35$, and $Z^* = 0.7$; and (d) $\chi_{zb} = 2.5$, $K = 35$, and $Z^* = 0.2$.

B. Effects of interaction parameter, equilibrium constant, and gelation criterion

To further illustrate the rich equilibrium states of the quaternary system, let us first fix $n = m = 1$, $v_x = v_y = 1$, $r_x = r_y = 1$, $r_z = v_z = 2$, and only vary the interaction parameter χ_{zb}, the equilibrium constant K, and the gelation threshold Z^*. Upon decreasing the repulsive interaction between Z and B, the two-phase coexistence region in Fig. 2(b) shrinks significantly in the direction perpendicular to the tie-lines and moves further away from the X-axis. Similarly, when the formation of the complex phase becomes less favorable chemically by decreasing the equilibrium constant K from 100 to 35, the two-phase coexistence region moves further away from the bottom left corner, as shown in Fig. 2(c), indicating that systems with a low overall concentration of formed complexes tend not to phase separate. In addition, we observe that the two-phase coexistence and gelation regions no longer overlap, indicating that all phase separated domains will remain liquid-like. On the contrary, in Fig. 2(d), with $Z^* = 0.2$, the entire right boundary of the two-phase coexistence region resides within the gelation region, indicating that all initial compositions inside the two-phase coexistence region lead to the formation of a gel (either confined to droplets or a system-spanning network as dictated by the volume fraction of Z). Note that it is also possible to form a gel network without phase separation if the initial composition is inside the single-phase gelation region. This can be done by initiating the system in the shaded-color region of the phase diagram.

C. Effects of stoichiometric coefficients

The effects of stoichiometric coefficients on coupled phase separation and gelation behavior of the system were also investigated by systematically varying n and m in the reaction between two small molecule species, defined by the constants $v_x = v_y = 1$, $r_x = r_y = 1$, and $r_z = v_z = nv_x + mv_y$. In addition, we set $Z^* = 0.4$ in all four cases shown in Fig. 3. Figure 3(a) shows the phase diagram of a symmetric case with $n = m = 1$. In Fig. 3(b), we consider a different stoichiometric ratio for the reaction between X and Y, namely, $n = 5$ and $m = 1$ ($5X + Y \leftrightarrow Z$). The two-phase coexistence region in the resulting phase diagram shows a clear asymmetric shape and also a different complex volume fraction distribution as compared

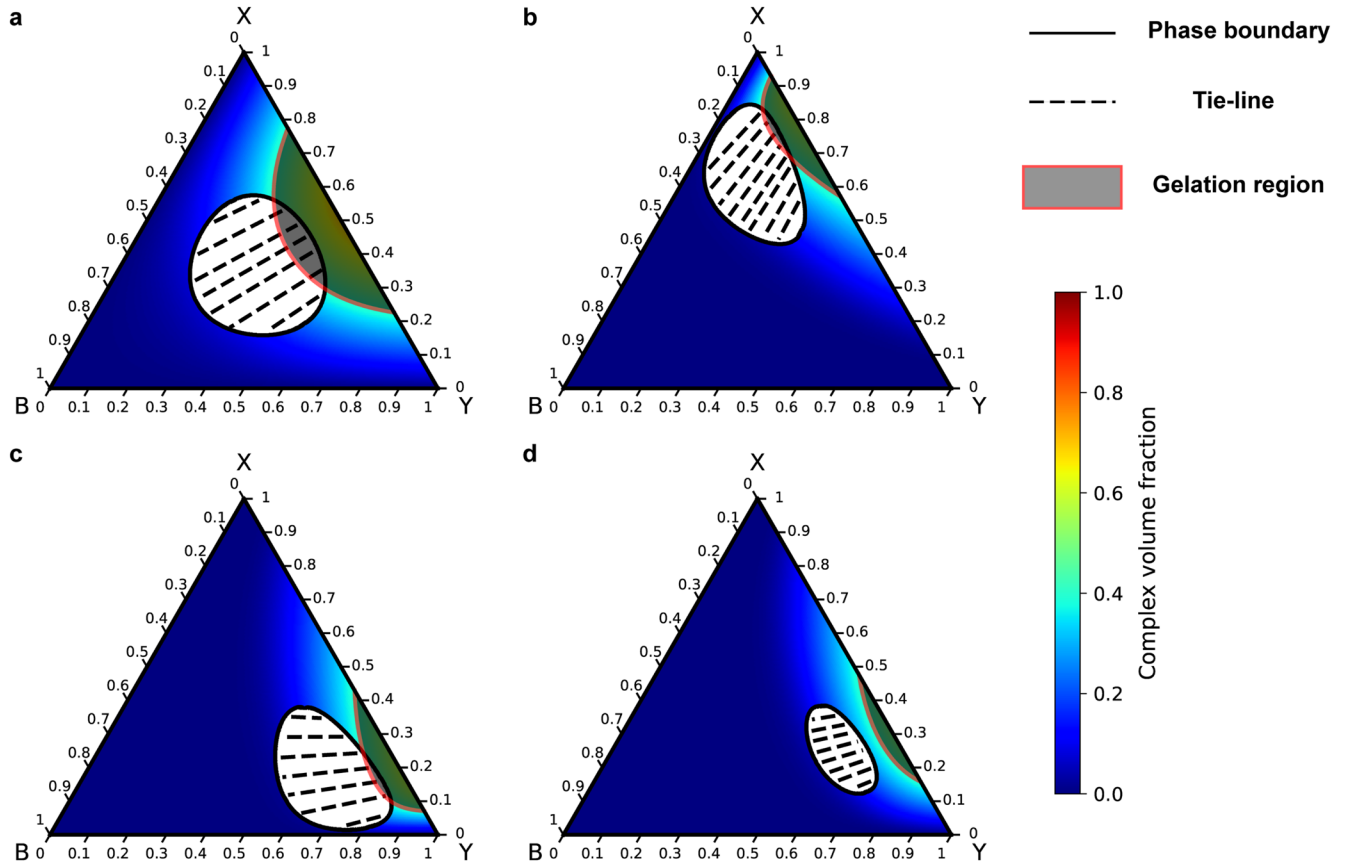

FIG. 3. Effects of varying stoichiometric coefficients of the reaction on the phase behavior of the quaternary mixture at fixed interaction and gelation parameters ($\chi_{zb} = 3$, $K = 10$, and $Z^* = 0.4$), molecular volumes ($v_x = v_y = 1$), and degrees of polymerization ($r_x = r_y = 1, r_z = v_z$). The stoichiometric coefficients were set to (a) $n = m = 1$; (b) $n = 5$ and $m = 1$; (c) $n = 1$ and $m = 5$; and (d) $n = 2$ and $m = 5$.

to the symmetric case in Fig. 3(a). This is simply due to the fact that in forming the complex, the system consumes more X than Y, and hence the phase diagram becomes skewed toward high X volume fractions. By setting $n = 1$ and $m = 5$, it yields a phase diagram that is mirrored by the line $X = Y$ [Fig. 3(c)]. Finally, changing the stoichiometric ratio to $n = 2$ and $m = 5$, gives rise to a phase diagram [cf. Fig. 3(d)] with a lower overall volume fraction of formed complexes.

D. Effects of molecular size and degree of polymerization

A system rich in multi-valent interactions normally shows size discrepancies among the different macromolecular species. Therefore, we proceed to study the effects of different molecular volumes and degrees of polymerization on the phase behavior of the system. When the molecular volume of one reactant species is larger than the other (e.g., $v_x \neq v_y$), the phase diagram is influenced by the product of the stoichiometric coefficient and molecular volume of each species, as described by Eq. (3). Despite representing different physical meanings, setting $n = 2$, $m = 5$, and $v_x = v_y = 1$ [cf. Fig. 3(d)] is mathematically indistinguishable from setting $n = 1$, $m = 5$, $v_x = 2$, and $v_y = 1$ (X represents a larger "blob" than Y) within the current formulation. Consequently, both cases will yield identical phase diagrams.

So far, the systems discussed have adhered to the constraint $r_z = v_z$, which is physically reasonable for the formation of extended chains or copolymers. However, it is possible that this constraint may be violated in multicomponent mixtures undergoing chemical reactions and phase separation. In fact, theoretical investigations have recognized the need to introduce corrections to lattice models to accommodate diverse polymer architectures.[34] Moreover, molecular simulations have suggested that condensate-forming proteins exhibit different conformations in dilute and dense phases due to sequence-specific intra-chain and inter-chain interactions.[35] Therefore, we next proceed to investigate the impact of the degree of polymerization by intentionally relaxing this constraint. More specifically, in Fig. 4, we show the resulting phase diagrams at fixed parameter values $n = 5$, $m = 1$, $v_x = 1$, $v_y = 5$, $r_x = r_y = 1$, $\chi_{zb} = 3$, $K = 35$, and $Z^* = 0.4$. In Fig. 4(a), we set $r_z = 6$ and $v_z = 10$, reflecting that the complex molecule has a more granular structure than extended polymers with the same molecular volume. The phase diagram is symmetric about $X = Y$, and we further discover that the

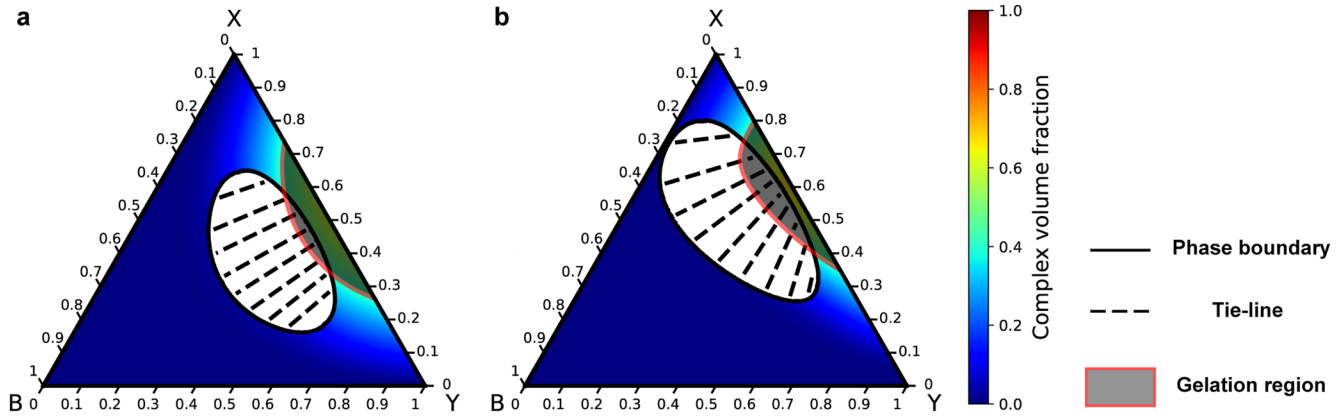

FIG. 4. Effects of varying molecular volumes and degrees of polymerization on the phase behavior of the quaternary mixture at fixed stoichiometric coefficients ($n = 5$ and $m = 1$) and interaction and gelation parameters ($\chi_{zb} = 3$, $K = 35$, and $Z^* = 0.67$). The volumes and degrees of polymerization of each species were set to (a) $v_x = 1$, $v_y = 5$, $v_z = 10$, $r_x = r_y = 1$, and $r_z = 6$. (b) $v_x = 1$, $v_y = 5$, $v_z = 10$, $r_x = 1$, $r_y = 5$, and $r_z = 8$.

coexistence region shrinks toward the X-axis as r_z increases, while it expands toward $B = 1$ as r_z decreases.

Next, we consider a more complex case where a long polymer Y with volume $v_y = 5$ reacts with five small X molecules with volume $v_x = 1$. The polymer also has a higher degree of polymerization than the small molecule, such that $r_x = 1$, $r_y = 5$, and the complex has an extended structure with $r_z = 8$. Compared to Fig. 4(a), the phase diagram in Fig. 4(b) demonstrates that increasing v_y not only expands the two-phase coexistence region but also causes it to become more skewed toward the X- and B-axes. It suggests that higher degrees of polymerization may facilitate LLPS and/or gelation at lower volume fractions of X and/or Y. This observation aligns with the experimental findings that phase boundaries of multi-valent protein mixtures can be shifted by increasing the degree of polymerization, which may also help induce a sol–gel transition.[36,37]

E. Spinodal behavior

LLPS may proceed either via nucleation and growth or spinodal decomposition. In the spinodal region, the mixture becomes globally unstable under small compositional fluctuations and results in spontaneous phase separation without nucleation. Identifying such regions is important for both numerical simulations and experiments.

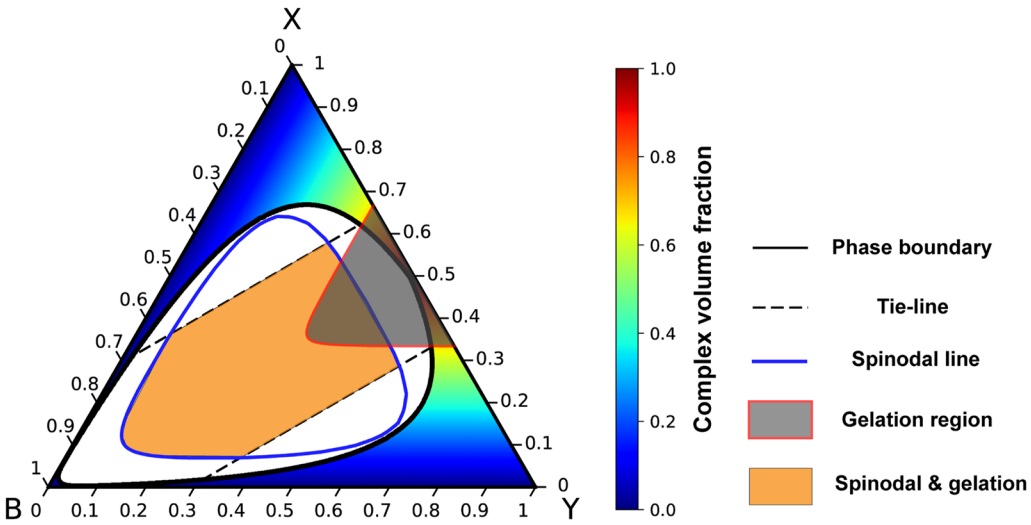

FIG. 5. Representative phase diagram with significantly overlapping spinodal and gelation regions. The parameter values employed in the construction of the phase diagram were set to $n = m = 1$, $v_x = v_y = 1$, $r_x = r_y = r_z = 1$, $\chi_{zb} = 4$, $K = 100$, and $Z^* = 0.67$. Even though the gelation region makes only a small "excursion" within the two-phase coexistence region, a significant fraction of the initial compositions within the spinodal would lead to phase separated gel-like domains.

Thus, in addition to the phase boundaries (binodal lines) displayed in the phase diagrams in Figs. 2–4, we have also determined the spinodal regions via a standard quadratic approximation. That is, for a given initial composition (X_0, Y_0), we expand f_{liquid} from Eq. (3) up to the second order in the compositional variations via $f_{\text{liquid}}(X, Y) \approx f_{\text{liquid}}(X_0, Y_0) + \vec{\nabla} f_{\text{liquid}}(X_0, Y_0) \cdot [X - X_0, Y - Y_0]^T + \frac{1}{2} [X - X_0, Y - Y_0] \cdot H_f \cdot [X - X_0, Y - Y_0]^T$, where $H_{f;i,j} = \frac{\partial^2 f_{\text{liquid}}}{\partial X_i \partial X_j}|_{X_0;Y_0}$ denotes the Hessian. The spinodal region is identified as the one wherein at least one of the two eigenvalues of H_f is negative. Having thus identified the thermodynamically unstable regions, we then delineate them in the phase diagram as shown in Fig. 5. We further identify inside the spinodal region the initial compositions where spinodal decomposition and gelation happen concurrently (colored orange). It is noteworthy that even though the gelation region makes only small "excursions" within the two-phase coexistence regions, a significant fraction of the initial compositions within the spinodal—those easily triggered to display phase separation either numerically or experimentally—would lead to phase separated gel-like domains.

IV. CONCLUSION

In this work, we have formulated a thermodynamic approach that incorporates chemical reactions in a non-ideal ternary macromolecular system and its propensity to undergo aging via gelation. We have shown that chemical reactions may significantly alter phase behavior when considering the effects of different stoichiometric coefficients, molecular sizes, degrees of polymerization, equilibrium constants, and interaction strengths. Clear asymmetries in the phase diagrams were observed for systems in which the stoichiometric coefficients, molecular volumes, and/or degrees of polymerization were significantly different between the two reactant molecular species. Furthermore, numerical identification of the spinodal regions demonstrated that in systems in which the gelation region overlaps with the two-phase coexistence one, large fractions of initial compositions within the spinodal regions would lead to phase separated gel-like domains.

With regard to the propensity of the system to undergo gelation, our analysis demonstrates that it can be effectively suppressed by (1) reducing the complex–buffer interaction parameter χ_{zb}, (2) decreasing the parameter K (corresponding to the equilibrium constant of the reaction in an ideal system), or (3) increasing the gelation threshold Z^*. It is noteworthy that the first two options would both weaken the driving force for phase separation and reduce the compositional contrast between the phases, thus possibly negatively impacting the biological functions of the domains. On the other hand, very recent experimental work has shown[38] that cross-linking may be tunable by ATP activity, thus providing a potential strategy for controlling the gelation threshold.

While the thermodynamic model developed in this paper is sufficiently general to allow for non-ideal behavior for the ternary X–Y-buffer system as well as gelation of the pure X or Y components, our choice of focusing on the phase separation of the complex Z from the buffer and its possible gelation was inspired by experimental observations of coacervate phase separation in protein–DNA-buffer systems,[11,12] in particular those in which neither the proteins nor DNA alone exhibited any macroscopic phase separation behavior in the buffer solution.[12] It would be interesting to extend the analysis herein to other systems in which the reactants may also display non-ideal solution and/or gelation behavior; we plan to address these questions in future work.

Finally, it is important to stress that for quantifying the full non-equilibrium behavior of phase-separating systems, which may or may not display aging, phase diagrams alone will not suffice; one has to resolve the full spatio-temporal kinetics of the molecular species and their aging behavior. To this end, we have implemented a thermodynamically consistent formulation of the kinetics, derived from an extension of Eq. (2) to spatially varying volume fractions and supplanted with appropriate mass conservation laws and reaction kinetics. This allows us to further generalize the N-component system to more complex scenarios in which reactants/products are not restricted to only one reaction. The detailed results, including numerical simulations and the interplay between kinetics and morphology, will appear in a separate paper.[27]

ACKNOWLEDGMENTS

R.Z. and M.P.H. were supported by the National Science Foundation (NSF) Materials Research Science and Engineering Center Program through the Princeton Center for Complex Materials (PCCM) (Grant No. DMR-2011750). S.M. acknowledges the partial support of the National Natural Science Foundation of China (NSFC) under Grant No. 12272005.

AUTHOR DECLARATIONS

Conflict of Interest

The authors have no conflicts to disclose.

Author Contributions

R.Z., S.M., and M.P.H. designed research, performed research, analyzed data and wrote the paper.

Ruoyao Zhang: Conceptualization (equal); Formal analysis (equal); Investigation (equal); Methodology (equal); Validation (equal); Visualization (equal); Writing – original draft (equal); Writing – review & editing (equal). **Sheng Mao**: Conceptualization (equal); Investigation (equal); Methodology (equal); Supervision (equal); Writing – review & editing (equal). **Mikko P. Haataja**: Conceptualization (equal); Funding acquisition (equal); Methodology (equal); Project administration (equal); Supervision (equal); Writing – review & editing (equal).

DATA AVAILABILITY

The data that support the findings of this study are available within the article.

APPENDIX: GENERALIZATION TO ARBITRARY NUMBER OF COMPONENTS

The generalization of our model to systems with even larger numbers of components is straightforward. To this end, consider an

N-component system (where N accounts for all molecular species present, including reactants, products, and un-reactive ones) with volume fractions φ_i subject to the incompressibility constraint $\sum_i^N \varphi_i = 1$. Here, the reactions are not restricted to binary ones, and we make the simplifying assumption that the reactants/products in one reaction do not react with other reactants/products. For M reversible reactions, we define an $M \times N$ stoichiometric matrix S_{ij}. Equation (1) then generalizes to

$$\sum_{j=1}^{N} S_{ij}\varphi_j = 0 \quad \text{for} \quad i = 1, \ldots, M, \tag{A1}$$

where the products (reactants) have positive (negative) entries for S_{ij}. Furthermore, let us define an $M \times N$ "participation matrix" P_{ij} such that $P_{ij} = 1$ if the jth component participates in the ith reaction and $P_{ij} = 0$ otherwise. Now, volume conservation is enforced via the M constraints,

$$\sum_{j=1}^{N} S_{ij}\nu_j = 0 \quad \text{for} \quad i = 1, \ldots, M. \tag{A2}$$

The free energy density in Eq. (2) then generalizes to

$$f_{\text{liquid}}(\{\varphi_j\}) = \sum_{j=1}^{N} \frac{\varphi_j}{r_j}\left(\ln \varphi_j + \mu_j^0\right) + \frac{1}{2}\sum_{j,k=1}^{N} \chi_{jk}\varphi_j\varphi_k, \tag{A3}$$

where, by convention, $\chi_{jk} = 0$ for $j = k$. Once the stoichiometric matrix S_{ij}, the interaction matrix χ_{jk}, and the standard chemical potentials μ_j^0 have been specified, phase diagrams can be constructed by following the procedure as in the quaternary system. That is, Eq. (3) can be generalized by introducing M reaction progress parameters γ_i for all distinct reactions,

$$\begin{aligned} f_{\text{liquid}}&\left(\{\varphi_j^0\}, \{\gamma_i\}\right) \\ &= \sum_{i=1}^{M}\sum_{j=1}^{N} P_{ij}\left\{\frac{\varphi_j^0 + S_{ij}\nu_j\gamma_i}{r_j}\left[\ln\left(\varphi_j^0 + S_{ij}\nu_j\gamma_i\right) + \mu_j^0\right]\right. \\ &\quad \left. + \frac{1}{2}\sum_{j,k=1}^{N} \chi_{jk}\left(\varphi_j^0 + S_{ij}\nu_j\gamma_i\right) \times \left(\varphi_k^0 + S_{ik}\nu_k\gamma_i\right)\right\} \\ &\quad + \sum_{i=1}^{M}\sum_{j=1}^{N} (1 - P_{ij})\left[\frac{\varphi_j^0}{r_j}\left(\ln \varphi_j^0 + \mu_j^0\right) + \frac{1}{2}\sum_{j,k=1}^{N} \chi_{jk}\varphi_j^0\varphi_k^0\right], \end{aligned} \tag{A4}$$

where φ_j^0 denotes the volume fraction of species j before mixing, thus the volume fractions of the products are initially zero. Subsequently, $\gamma_{i,\min}$ can be computed by minimizing $f_{\text{liquid}}\left(\{\varphi_j^0\}, \{\gamma_i\}\right)$ with respect to the γ_i with ease as the reactions are non-interfering with one another. The phase diagram can be calculated using the same procedures as discussed in Sec. III. Although the convex hull construction is conceptually straightforward, it is computationally challenging for higher-dimensional systems, e.g., $N > 6$.[22]

REFERENCES

[1] C. P. Brangwynne, C. R. Eckmann, D. S. Courson, A. Rybarska, C. Hoege, J. Gharakhani, F. Jülicher, and A. A. Hyman, "Germline P granules are liquid droplets that localize by controlled dissolution/condensation," Science **324**, 1729–1732 (2009).

[2] A. A. Hyman, C. A. Weber, and F. Jülicher, "Liquid-liquid phase separation in biology," Annu. Rev. Cell Dev. Biol. **30**, 39–58 (2014).

[3] Y. Shin and C. P. Brangwynne, "Liquid phase condensation in cell physiology and disease," Science **357**, eaaf4382 (2017).

[4] L. Jawerth, E. Fischer-Friedrich, S. Saha, J. Wang, T. Franzmann, X. Zhang, J. Sachweh, M. Ruer, M. Ijavi, S. Saha, J. Mahamid, A. A. Hyman, and F. Jülicher, "Protein condensates as aging Maxwell fluids," Science **370**, 1317–1323 (2020).

[5] M. Jucker and L. C. Walker, "Self-propagation of pathogenic protein aggregates in neurodegenerative diseases," Nature **501**, 45–51 (2013).

[6] T. Lu and E. Spruijt, "Multiphase complex coacervate droplets," J. Am. Chem. Soc. **142**, 2905–2914 (2020).

[7] C. E. Sing and S. L. Perry, "Recent progress in the science of complex coacervation," Soft Matter **16**, 2885–2914 (2020).

[8] D. Bracha, M. T. Walls, M.-T. Wei, L. Zhu, M. Kurian, J. L. Avalos, J. E. Toettcher, and C. P. Brangwynne, "Mapping local and global liquid phase behavior in living cells using photo-oligomerizable seeds," Cell **175**, 1467–1480.e13 (2018).

[9] W. C. K. Poon, "The physics of a model colloid polymer mixture," J. Phys.: Condens. Matter **14**, R859–R880 (2002).

[10] A. Radhakrishnan and H. M. McConnell, "Condensed complexes of cholesterol and phospholipids," Biophys. J. **77**, 1507–1517 (1999).

[11] H. Zhou, Z. Song, S. Zhong, L. Zuo, Z. Qi, L.-J. Qu, and L. Lai, "Mechanism of DNA-induced phase separation for transcriptional repressor VRN1," Angew. Chem., Int. Ed. **58**, 4858–4862 (2019).

[12] J.-K. Ryu, C. Bouchoux, H. W. Liu, E. Kim, M. Minamino, R. de Groot, A. J. Katan, A. Bonato, D. Marenduzzo, D. Michieletto, F. Uhlmann, and C. Dekker, "Bridging-induced phase separation induced by cohesin SMC protein complexes," Sci. Adv. **7**, eabe5905 (2021).

[13] L. C. M. Mackinder, M. T. Meyer, T. Mettler-Altmann, V. K. Chen, M. C. Mitchell, O. Caspari, E. S. Freeman Rosenzweig, L. Pallesen, G. Reeves, A. Itakura, R. Roth, F. Sommer, S. Geimer, T. Mühlhaus, M. Schroda, U. Goodenough, M. Stitt, H. Griffiths, and M. C. Jonikas, "A repeat protein links rubisco to form the eukaryotic carbon-concentrating organelle," Proc. Natl. Acad. Sci. U. S. A. **113**, 5958–5963 (2016).

[14] S. He, H.-T. Chou, D. Matthies, T. Wunder, M. T. Meyer, N. Atkinson, A. Martinez-Sanchez, P. D. Jeffrey, S. A. Port, W. Patena, G. He, V. K. Chen, F. M. Hughson, A. J. McCormick, O. Mueller-Cajar, B. D. Engel, Z. Yu, and M. C. Jonikas, "The structural basis of rubisco phase separation in the pyrenoid," Nat. Plants **6**, 1480–1490 (2020).

[15] L. R. Corrales and J. C. Wheeler, "Chemical reaction driven phase transitions and critical points," J. Chem. Phys. **91**, 7097–7112 (1989).

[16] V. Talanquer, "Global phase diagram for reacting systems," J. Chem. Phys. **96**, 5408–5421 (1992).

[17] H. M. McConnell and A. Radhakrishnan, "Condensed complexes of cholesterol and phospholipids," Biochim. Biophys. Acta, Biomembr. **1610**, 159–173 (2003).

[18] A. Radhakrishnan and H. McConnell, "Condensed complexes in vesicles containing cholesterol and phospholipids," Proc. Natl. Acad. Sci. U. S. A. **102**, 12662–12666 (2005).

[19] M. Z. Bazant, "Theory of chemical kinetics and charge transfer based on nonequilibrium thermodynamics," Acc. Chem. Res. **46**, 1144–1160 (2013).

[20] M. Z. Bazant, "Thermodynamic stability of driven open systems and control of phase separation by electro-autocatalysis," Faraday Discuss. **199**, 423–463 (2017).

[21] J. Kirschbaum and D. Zwicker, "Controlling biomolecular condensates via chemical reactions," J. R. Soc. Interface **18**, 20210255 (2021).

[22] S. Mao, D. Kuldinow, M. P. Haataja, and A. Košmrlj, "Phase behavior and morphology of multicomponent liquid mixtures," Soft Matter **15**, 1297–1311 (2019).

[23]T. Tanaka, G. Swislow, and I. Ohmine, "Phase separation and gelation in gelatin gels," Phys. Rev. Lett. **42**, 1556–1559 (1979).
[24]A. Patel, H. O. Lee, L. Jawerth, S. Maharana, M. Jahnel, M. Y. Hein, S. Stoynov, J. Mahamid, S. Saha, T. M. Franzmann, A. Pozniakovski, I. Poser, N. Maghelli, L. A. Royer, M. Weigert, E. W. Myers, S. Grill, D. Drechsel, A. A. Hyman, and S. Alberti, "A liquid-to-solid phase transition of the ALS protein FUS accelerated by disease mutation," Cell **162**, 1066–1077 (2015).
[25]T. R. Peskett, F. Rau, J. O'Driscoll, R. Patani, A. R. Lowe, and H. R. Saibil, "A liquid to solid phase transition underlying pathological huntingtin Exon1 aggregation," Mol. Cell **70**, 588–601.e6 (2018).
[26]J. Berry, C. P. Brangwynne, and M. Haataja, "Physical principles of intracellular organization via active and passive phase transitions," Rep. Prog. Phys. **81**, 046601 (2018).
[27]R. Zhang, S. Mao, and M. Haataja, "Chemically reactive and aging macromolecular mixtures II: Phase separation and coarsening," J. Chem. Phys. (2024) (submitted).
[28]F. Tanaka, "Theory of thermoreversible gelation," Macromolecules **22**, 1988–1994 (1989).
[29]F. Sciortino, R. Bansil, H. E. Stanley, and P. Alstrøm, "Interference of phase separation and gelation: A zeroth-order kinetic model," Phys. Rev. E **47**, 4615–4618 (1993).
[30]R. Horst and B. A. Wolf, "Phase diagrams calculated for quaternary polymer blends," J. Chem. Phys. **103**, 3782–3787 (1995).
[31]S. L. Veatch and S. L. Keller, "Separation of liquid phases in giant vesicles of ternary mixtures of phospholipids and cholesterol," Biophys. J. **85**, 3074–3083 (2003).
[32]J. Wolff, C. M. Marques, and F. Thalmann, "Thermodynamic approach to phase coexistence in ternary phospholipid-cholesterol mixtures," Phys. Rev. Lett. **106**, 128104 (2011).
[33]M. Harper *et al.*, "python-ternary: Ternary plots in python," Zenodo. https://doi.org/10.5281/zenodo.594435
[34]A. M. Nemirovsky, M. G. Bawendi, and K. F. Freed, "Lattice models of polymer solutions: Monomers occupying several lattice sites," J. Chem. Phys. **87**, 7272–7284 (1987).
[35]M. Farag, S. R. Cohen, W. M. Borcherds, A. Bremer, T. Mittag, and R. V. Pappu, "Condensates formed by prion-like low-complexity domains have small-world network structures and interfaces defined by expanded conformations," Nat. Commun. **13**, 7722 (2022).
[36]P. Li, S. Banjade, H.-C. Cheng, S. Kim, B. Chen, L. Guo, M. Llaguno, J. V. Hollingsworth, D. S. King, S. F. Banani, P. S. Russo, Q.-X. Jiang, B. T. Nixon, and M. K. Rosen, "Phase transitions in the assembly of multivalent signalling proteins," Nature **483**, 336–340 (2012).
[37]T. Mittag and R. V. Pappu, "A conceptual framework for understanding phase separation and addressing open questions and challenges," Mol. Cell **82**, 2201–2214 (2022).
[38]S. Coupe and N. Fakhri, "Atp-induced cross-linking of a biomolecular condensate," Biophys. J. **123**, 1–11 (2023).